Differential excitation cross sections of molecular oxygen by electron impact: The longest and second bands

Tong W. Shyn, Christopher J. Sweeney, and Alan Grafe
Space Physics Research Laboratory, University of Michigan, Ann Arbor, Michigan 48109-2143
(Received 22 November 1993)

We have measured absolute differential excitation cross sections for the longest and second bands of molecular oxygen by electron impact. A crossed-beam method was used. The angular range covered was 12° to 156°, while the impact energy range was 15 to 50 eV. Two pronounced minima are present in the angular distributions of both cross sections, indicating in both cases substantial *D*-wave character. Additionally, the angular distributions show that both the longest and second bands are composite structures, arising from a combination of electric dipole allowed and electric dipole forbidden transitions. We also computed integrated cross sections from the present differential cross sections, and found a broad maximum in the former near 20-eV impact.

PACS number(s): 34.80.Gs

I. INTRODUCTION

One of the most important constituents of the Earth's atmosphere is molecular oxygen. It is essential in the biological process of respiration, and participates in such phenomena as the atmospheric nightglow and the energy-loss process of electrons traversing the atmosphere. Consequently, information regarding fundamental aspects of this molecule is vital to researchers in many branches of science.

Molecular oxygen has been the subject of much research, and as the excellent reviews by Hudson [1], Krupenie [2], and Itikawa *et al.* [3] show, substantial progress has been made in understanding its structure and dynamics. However, our knowledge of the low-energy (i.e., less than 100-eV incident energy) electron-impact excitation of the longest (LB) and second (2B) bands of O_2, two features in the energy-loss spectrum located at excitation energies of 9.97 and 10.29 eV, respectively, is still quite limited. Angular differential excitation cross sections for these features provide information vital for the identification of state character, and in addition are important to those who model the Earth's atmosphere.

Several electron-impact experiments concerning the LB and 2B have been undertaken over a variety of angular and impact energy ranges. For purely forward scattering, investigations have been done by Geiger and Schröder [4] with 25-keV electrons, and by Huebner *et al.* [5] with 100-eV electrons. Lassettre, Silverman, and Krasnow [6] considered small-angle scattering, covering angles less than 10° and using an impact energy of 518 eV. Trajmar, Williams, and Kuppermann [7] obtained approximately normalized electron-impact excitation cross sections for the LB and 2B over the angular range 10° through 90° at 20- and 45-eV impact energy. Based on the angular dependence of these cross sections and the optical data obtained by Tanaka [8] and Ogawa and Yamawaki [9], they concluded that the LB and 2B are due mostly to the electric dipole allowed transitions $^3\Sigma_u^- \leftarrow X\,^3\Sigma_g^-$ or $^3\Pi_u \leftarrow X\,^3\Sigma_g^-$. Wakiya [10] measured relative electron-impact excitation cross sections for the entire energy-loss region from 9.7 through 12.1 eV, which includes the LB and 2B. He covered the angular range 5° to 130° and the impact energy range 20 to 100 eV. To date the only absolute electron-impact cross section measurements are those of Newell, Khakoo, and Smith [11], who covered the angular range 5° to 40° and the incident energy region 100 to 500 eV. Their measurements led them to conclude that the LB and 2B are composite in nature, arising from both electric dipole allowed and electric dipole forbidden transitions.

There have been several theoretical studies of the state character of the LB and 2B. Lindholm [12] employed quantum defect arguments to suggest that the LB and 2B correspond to the third and fourth vibrational levels of the $^3\Sigma_u^-$ electronic state. (In contrast to this, Tanaka [8] suggested from the pressure broadening he observed with optical experiments that the LB and 2B arise from different electronic transitions.) Using the virtual orbital technique, Cartwright *et al.* [13] calculated the LB to be at an excitation energy of 9.98 eV, and assigned it to the $^3\Pi_u$ Rydberg state. In contrast to this, however, Yoshimine *et al.* [14] performed configuration-interaction calculations and proposed that the LB and 2B arise from the $^3\Sigma_u^-$ ($v=0,1$) Rydberg state. They located the excitation energies for the LB and 2B at 9.96 and 10.29 eV, respectively. Buenker and Peyerimhoff [15], employing configuration-interaction calculations, posited the existence of two $^3\Pi_u$ states in the energy excitation region of the LB and 2B, one with a shoulder in its potential energy curve near 9.0 eV and the other with an excitation energy of 10.75 eV.

In this paper we present the results of absolute electron-impact differential excitation cross-section measurements for the LB and 2B of molecular oxygen. A crossed-beam method was employed. The impact energy and angular ranges covered were 15 to 50 eV and 12° to 156°, respectively. The angular shapes of both cross sections indicate that the LB and 2B are composite struc-

tures, originating from both electric dipole allowed and electric dipole forbidden transitions. Substantial *D*-wave character was observed in both cases. From our measured results we computed integrated cross sections; the latter exhibit a maximum near 20-eV impact energy.

II. EXPERIMENT

The apparatus and procedures we employed were essentially the same as those used in other recent O_2 measurements by two of the present authors [16,17], and are given detailed accounts elsewhere [18,19]. Therefore we here include only a brief discussion. Three principal subsystems comprise our apparatus: a neutral-molecular-oxygen-beam source, a monoenergetic electron-beam source, and a scattered electron detector. All three reside in a twin chamber, differentially pumped vacuum system. Magnetic fields within the interaction region of this vacuum system are limited to 20 mG in all directions by three sets of mutually perpendicular Helmholtz coils. The energy scale was calibrated against the 19.3-eV resonance of helium.

The neutral-molecular-oxygen-beam source is located in the upper vacuum chamber. Research grade O_2 is piped into this chamber. The piping terminates at a capillary array positioned at the junction between the two chambers, providing a collimated molecular beam which in the lower chamber intersects the horizontal plane of the electron-beam source and detector.

The electron-beam source can be rotated continuously from $-90°$ to 160°. It consists of an electron gun with a thoria-coated iridium filament, a cylindrical energy selector, two electron lenses, and two beam deflectors. Currents exceeding 10^{-8} A are produced by this system. The beam's divergence angle is less than $\pm 3°$ full width at half maximum (FWHM), while its energy resolution is about 80 meV FWHM.

Fixed to the lower chamber wall is the scattered electron detector. It is made of cylindrical and hemispherical energy analyzers in tandem, two electron lenses, and a Channeltron electron multiplier. A solid angle of detection of about 5×10^{-4} sr is afforded by this system, while its energy resolution is better than 60 meV FWHM. This dual-analyzer system provides a signal-to-noise ratio more than 100 times superior to our previous single-analyzer system.

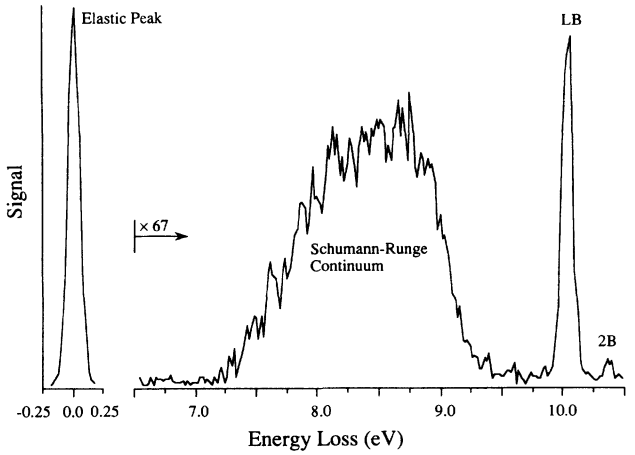

FIG. 1. A typical energy-loss spectrum for molecular oxygen. The scattering angle is 72°, while the impact energy is 20 eV. Clearly visible are narrow peaks corresponding to elastic scattering and excitation to the LB and 2B. A broad band corresponding to excitation to the Schumann-Runge continuum is also present. Note the change in scale by a factor of 67 in the right portion of the spectrum.

Both the electron-beam source and detector are under the control of a dedicated microcomputer. During the measurement process this computer maintains the electron-beam energy constant, while sweeping the acceptance energy of the detector repeatedly over the region of interest. The results are energy-loss spectra like that shown in Fig. 1, which is for an impact energy of 20 eV, and a scattering angle of 72°. Apparent in this figure are three narrow peaks, along with a fairly wide band. The

TABLE I. Absolute excitation cross sections of molecular oxygen measured by electron impact. Parentheses enclose extrapolated values. (a) The longest band (LB). Units for the differential cross sections are 10^{-19} cm^2/sr, while those for the integrated cross sections are 10^{-18} cm.^{2} (b) The second band (2B). Units for the differential cross sections are 10^{-20} cm^2/sr, while those for the integrated cross sections are 10^{-19} cm^2.

E (eV) \ θ (deg)	12	24	36	48	60	72	84	96	108	120	132	144	156	168	σ_i
							(a) LB								
15	24.6	17.4	8.97	4.00	2.73	1.84	2.74	2.70	2.55	3.14	3.29	3.52	4.32	(5.60)	5.75
20	51.4	23.1	8.56	3.36	2.42	2.39	2.86	2.55	2.23	2.10	2.82	4.01	5.45	(6.80)	6.69
30	72.5	20.7	4.03	1.32	2.09	2.52	1.92	1.38	1.26	1.65	2.66	4.28	5.95	(8.34)	6.22
50	35.1	3.68	0.61	1.05	1.02	0.62	0.31	0.12	0.22	0.47	0.99	2.11	3.57	(4.90)	2.36
							(b) 2B								
15	39.1	32.3	13.1	6.60	2.40	2.10	2.10	1.90	2.20	2.50	2.80	3.30	4.90	(6.00)	7.20
20	136	40.0	10.0	2.90	2.00	1.80	2.00	2.00	1.20	1.20	1.60	3.00	4.60	(6.00)	9.15
30	150	32.8	3.10	1.40	1.67	1.82	1.16	0.87	0.89	0.76	1.43	2.78	3.97	(5.82)	8.71
50	121	6.10	1.30	1.60	1.10	0.70	0.30	0.14	0.30	0.60	1.02	1.45	1.89	(2.50)	4.72

leftmost peak corresponds to elastic scattering, while the central and rightmost correspond to excitation of the LB and 2B of O_2, respectively. The wide band corresponds to excitation of O_2 to the Schumann-Runge continuum.

We conducted our measurement process over the prescribed range of impact energies and scattering angles. Results were placed on an absolute scale by normalizing signal strengths to the absolute elastic O_2 scattering cross sections measured by one of the present authors [20]. Detector efficiency as a function of energy loss was accounted for during this procedure.

III. DISCUSSION OF RESULTS

Measured values for absolute LB and 2B differential excitation cross sections (DCS's), along with integrated cross sections (ICS's) calculated from these values, are presented in Table I. The statistical uncertainty in the data was better than $\pm 10\%$ for the LB and $\pm 15\%$ for the 2B. Additional contributions to the uncertainty in the DCS's are $\pm 10\%$ due to the detector efficiency and $\pm 14\%$ for the elastic scattering DCS's used for normalization of the present results. When combined, these yield $\pm 20\%$ uncertainty in the LB DCS's and $\pm 23\%$ in the 2B DCS's.

ICS's were computed from the DCS's by means of the trapezoid rule. This required that we extrapolate the DCS's to both 0° and 180°, which we did in semiexponential fashion. As the DCS's are strongly forward peaked, special consideration was given to low angles. For these we extrapolated in 3° increments below 24°. Due to the smallness of the factor $\sin\theta$ in the integral at such angles, an error of less than $\pm 3\%$ may be introduced into the ICS's. The overall uncertainties in the ICS's are therefore comparable to those of the corresponding DCS's.

Figure 2 displays our measured values for the LB DCS's at 15 and 20 eV, along with the results of Trajmar, Williams, and Kuppermann at 20 eV. Our 15-eV results show strong forward scattering, accompanied by relatively isotropic scattering at middle and high angles. Such an angular distribution indicates that at least one electric dipole allowed and one electric dipole forbidden transition are involved in the production of the LB, just as determined by Newell, Khakoo, and Smith. Slight *D*-wave character is suggested by our 15-eV results, with minima occurring near 75° and 105°. This *D*-wave character becomes more pronounced in our 20-eV results, with minima at approximately 75° and 120°. The results of Trajmar, Williams, and Kuppermann at 20 eV agree with the present results in angular distribution, but their results are smaller in magnitude than ours. As mentioned previously, their normalization scheme was only approximate. This may account for the differences in magnitude among our results and theirs.

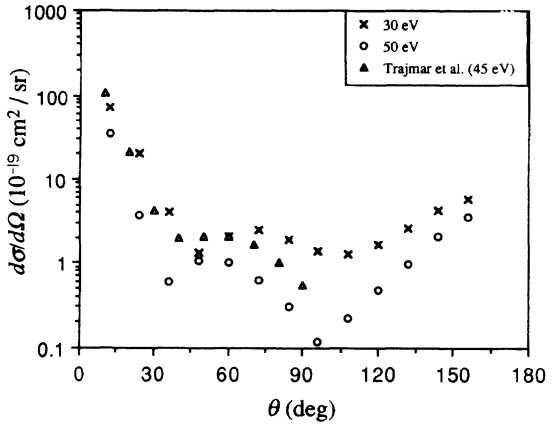

FIG. 3. Differential excitation cross sections for the LB of molecular oxygen at 30 and 50 eV, along with the results of Trajmar, Williams, and Kuppermann at 45 eV.

In Fig. 3 are shown our DCS's for excitation to the LB at 30 and 50 eV, along with those of Trajmar, Williams, and Kuppermann at 45 eV. At 30- and 50-eV impact, our results have minima near 45° and 105°, and 30° and 90°, respectively. Additionally, the *D*-wave character is more pronounced than for our 15- and 20-eV results. The angular distribution of the results of Trajmar, Williams, and Kuppermann at 45 eV agrees with the present

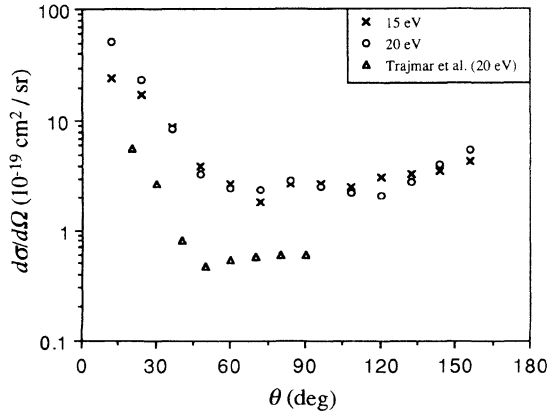

FIG. 2. Differential excitation cross sections for the LB of molecular oxygen at 15 and 20 eV, along with the results of Trajmar, Williams, and Kuppermann at 20 eV.

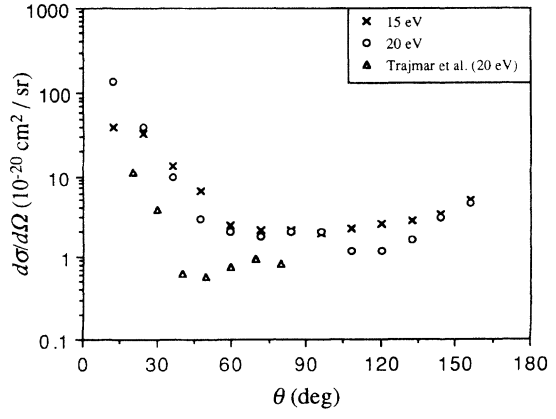

FIG. 4. Differential excitation cross sections for the 2B of molecular oxygen at 15 and 20 eV, along with the results of Trajmar, Williams, and Kuppermann at 20 eV.

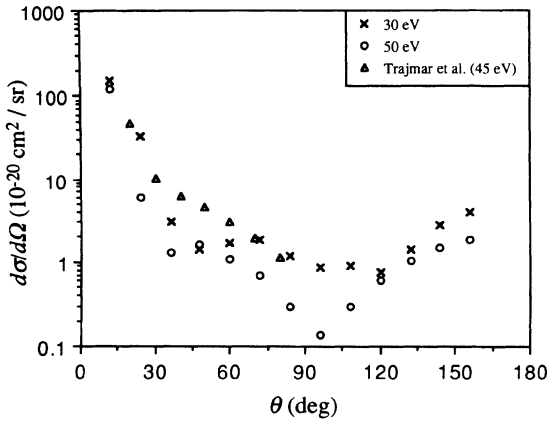

FIG. 5. Differential excitation cross sections for the 2B of molecular oxygen at 30 and 50 eV, along with the results of Trajmar, Williams, and Kuppermann at 45 eV.

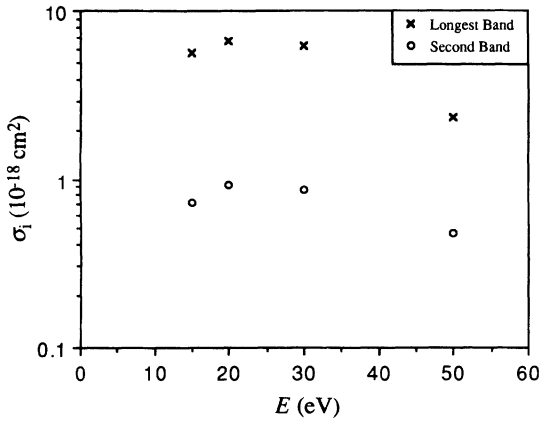

FIG. 6. Integrated cross sections for the LB and 2B of molecular oxygen.

results at 50 eV.

Figure 4 depicts our measured DCS's for the 2B at 15 and 20 eV, along with the results of Trajmar, Williams, and Kuppermann at 20 eV. Qualitatively, the angular distributions for the 2B are similar in character to those for the LB. This indicates that the 2B is composite in nature, again in agreement with the conclusions of Newell, Khakoo, and Smith. Only a hint of *D*-wave character is present in the 15-eV measurements, with minima near 75° and 105°. Somewhat more *D*-wave character is apparent in our 20-eV impact results, with minima occurring at approximately 60° and 120°. The approximately normalized results of Trajmar, Williams, and Kuppermann at 20 eV also exhibit a minimum, but near 45°.

In Fig. 5 our 30- and 50-eV DCS's for the 2B, along with the 45-eV 2B measurements of Trajmar, Williams, and Kuppermann, are presented. Here the minima in our results occur at about 45° and 120°, and 30° and 90°, for 30 and 50 eV, respectively. The results of Trajmar, Williams, and Kuppermann at 45 eV agree with the present results at 50 eV in angular distribution.

Figure 6 shows our results for the integrated cross sections for the LB and 2B. Both exhibit a broad maximum near 20-eV impact. The results of Trajmar, Williams, and Kuppermann are not shown because of their approximate normalization scheme and large uncertainty in extrapolation to 180° for obtaining these integrated cross sections.

IV. CONCLUSION

Using a crossed-beam method, we have measured absolute differential cross sections for excitation of the longest and second bands of O_2 by electron impact. Our measurements covered the relatively wide angular range of 12° to 156°, and the impact energy range of 15 through 50 eV.

Two minima are apparent in the angular distributions, indicating *D*-wave character. It is noteworthy that both minima approach smaller angles as the incident energy increases. Additionally, both strong forward scattering and relatively isotropic scattering at middle and high angles are present, indicating that both electric dipole allowed and electric dipole forbidden transitions are involved in the production of the longest and second bands. This is in agreement with the previous conclusions of Newell, Khakoo, and Smith.

We also calculated integrated cross sections from the differential cross sections. The former exhibit a broad resonance near 20-eV impact.

ACKNOWLEDGMENT

This research was supported by the National Science Foundation under Grants No. ATM-8913022 and No. ATM-9205041.

[1] R. D. Hudson, Rev. Geophys. Space Phys. **9**, 305 (1971).
[2] P. H. Krupenie, J. Phys. Chem. Ref. Data **1**, 423 (1972).
[3] Y. Itikawa, A. Ichimura, K. Onda, K. Sakimoto, K. Takayanagi, Y. Hatano, M. Hayashi, H. Nishimura, and S. Tsurubuchi, J. Phys. Chem. Ref. Data **18**, 23 (1989).
[4] J. Geiger and B. Schröder, J. Chem. Phys. **49**, 740 (1968).
[5] R. H. Huebner, R. J. Celotta, S. R. Mielczarek, and C. E. Kuyatt, J. Chem. Phys. **63**, 241 (1975).
[6] E. N. Lassettre, S. M. Silverman, and M. E. Krasnow, J. Chem. Phys. **40**, 1261 (1964).
[7] S. Trajmar, W. Williams, and A. Kuppermann, J. Chem. Phys. **56**, 3759 (1972).
[8] Y. Tanaka, J. Chem. Phys. **20**, 1728 (1952).
[9] M. Ogawa and K. R. Yamawaki, Can. J. Phys. **47**, 1805 (1969).
[10] K. Wakiya, J. Phys. B **11**, 3913 (1978).
[11] W. R. Newell, M. A. Khakoo, and A. C. H. Smith, J. Phys. B **13**, 4877 (1980).
[12] E. Lindholm, Ark. Fys. **40**, 117 (1969).
[13] D. C. Cartwright, W. J. Hunt, W. Williams, S. Trajmar, and W. A. Goddard III, Phys. Rev. A **8**, 2436 (1973).
[14] M. Yoshimine, K. Tanaka, H. Tatewaki, S. Obara, F.

Sasaki, and K. Ohno, J. Chem. Phys. **64**, 2254 (1976).
[15] R. J. Buenker and S. D. Peyerimhoff, Chem. Phys. Lett. **34**, 225 (1975).
[16] T. W. Shyn and C. J. Sweeney, Phys. Rev. A **47**, 1006 (1993).
[17] T. W. Shyn and C. J. Sweeney, Phys. Rev. A **48**, 1214 (1993).
[18] T. W. Shyn, R. S. Stolarski, and G. R. Carignan, Phys. Rev. A **6**, 1002 (1972).
[19] T. W. Shyn and T. E. Cravens, J. Phys. B **23**, 293 (1990).
[20] T. W. Shyn and W. E. Sharp, Phys. Rev. A **26**, 1369 (1982).